Supporting Information

Controlled synthesis of porous Co_3O_4-C hybrid nanosheet arrays and their application in lithium ion batteries

Jun Wang,[a,b] Bing Gao[a], Long Zhang[b], Rui Li[b], Jinpeng Shen[b], Zhiqiang Qiao[a], Guangcheng Yang *[a, b] and Fude Nie[a]

Received (in XXX, XXX) Xth XXXXXXXXX 20XX, Accepted Xth XXXXXXXXX 20XX
DOI: 10.1039/b000000x

[a] Institute of Chemical Materials, China Academy of Engineering Physics, Mianyang, 621900, Sichuan, China

[b] Sichuan New Material Research Center, Mianyang,621000, China

The formation of Co_3O_4 nanosheets (NS) is also verified by the FTIR result, as shown in Figure S1. In precursor, strong absorptions are observed in the 2850-2950 cm^{-1} range, corresponding to C-H bands, and at 1050-1125 cm^{-1}, corresponding to (CH_2), (C-O) bands. The precursor contains stretching vibrations bands of Co-O (519 cm^{-1}) and Co-OH (973 cm^{-1}). The band at 1624 cm^{-1} corresponds to the angular deformation of molecular water. After annealing at 450 °C for 2 h in N_2 flow, the bands of the precursor disappeared and two very strong peaks centered at 576 cm^{-1} and 672 cm^{-1} characteristic of spinel Co_3O_4. For both FTIR curves of the precursor and the obtained Co_3O_4, the broad band between 3440 cm^{-1} and 3500 cm^{-1}, could be assigned to the OH stretching and bending modes of water and surface hydroxyl groups.

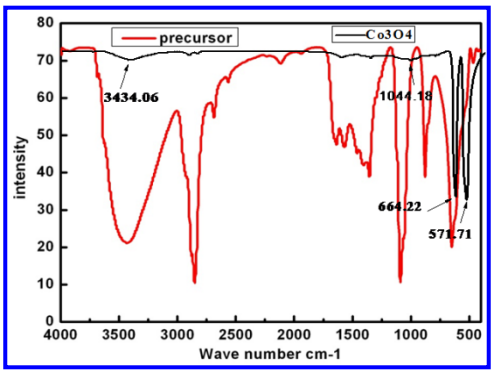

Figure S1. The FTIR spectra of the precursor and the products after annealing

The Raman spectrum of the products measured at room temperature in Figure S2 displays four Raman peaks located at around 476, 525, 622, and 692 cm^{-1}, respectively corresponding to the Eg, F2g, F2g, and A1g modes of the spinel Co_3O_4 phase. The Raman spectrum further demonstrates that the as-synthesized product is cobalt oxide.

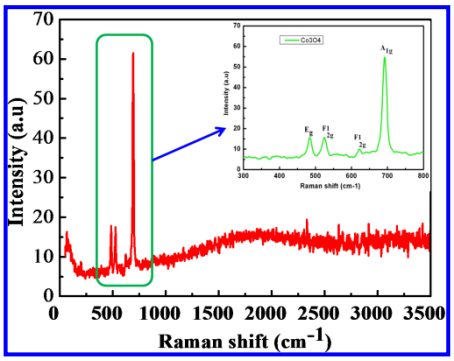

Figure S2. Raman spectrum of the products after annealing

It is important to control carbon content for improving electrochemical properties of electrode materials for lithium-ion batteries, because the carbon would provide a flexible buffer to accommodate the volume change during lithium insertion/extraction and increase the conductivity of the electrode. In this work, the carbon content of Co_3O_4-C NS can be controllable synthesized through controlling PVP content in the precursors and the conditions of the annealing. As shown in Figure. S3(a)-(c), the carbon content ranges from 21.30 % to 5.30 % with PVP concentration decreases from 0.8 to 0.5 g and the time of annealing increases from 2 to 4h.

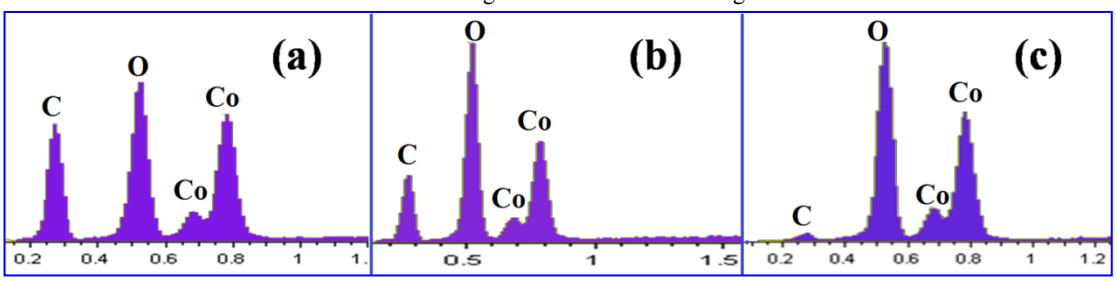

Figure S3 EDX elemental intensity of the NS arrays with different carbon content

Electrochemical capacities:

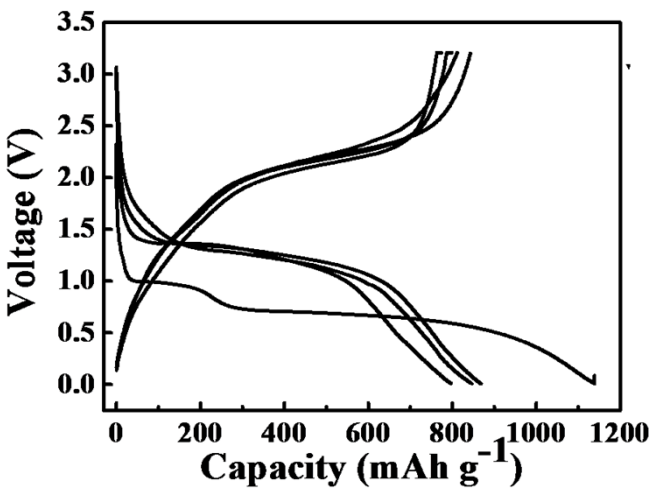

Figure. 4S the charge-discharge curves of Co_3O_4-C NS arrays for different cycles, the carbon content of the Co_3O_4-C NS is 16.5% and the mass of the electrode material is 2.94mg.

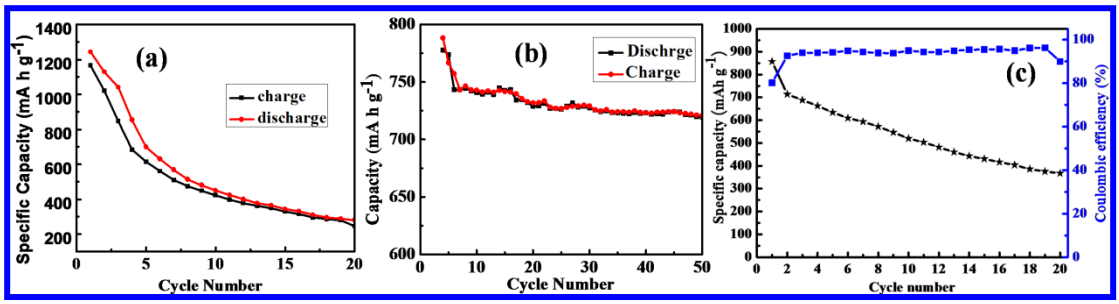

Figure. 5S (a): Figure. 5S (a): The capacity of the commercial Co_3O_4 sample.(b): The capacity of Co_3O_4-C nanosheet array. (c) The capacity of Co_3O_4/C nanocomposites.

Figure.5S(a) shows the cycling performance of the commercial Co_3O_4 sample between0.1 and 3.2 V at 0.2 C. The Co_3O_4 nanoparticles fades quickly, retains only 280 mA h g^{-1} after 20 cycles. The commercial Co_3O_4nanoparticles deliver an initial discharge capacity of 1124 mA h g^{-1} and exhibit a poor capacity retention with obvious capacity fading.

Figure. 5S(b) shows the charge specific capacity and the columbic efficiency with cycling at a current rate of C/2. It is evident that Co_3O_4-C nanosheet array shows much good cycling performance. The capacity of Co_3O_4-C nanosheet array remain as high as 720 mA h g^{-1} after 50 cycles, and the corresponding fading rate is 1.2% per cycle. The results reveal that Co_3O_4-C nanosheet array is really helpful for construction of Co_3O_4 anode materials with high LIB performance.

Figure. 5S(c) shows the cycling performance of the Co_3O_4/carbon nanocomposites. The Co_3O_4/carbon fades quickly, retains only 430 mA h g^{-1} after 20 cycles. The Co_3O_4/carbon deliver an initial discharge capacity of 860mA h g^{-1} and exhibit a poor capacity retention compared with Co_3O_4-C nanosheet array.

Table S1. List of lithium battery performance of Co_3O_4 from different references.

Reference	Nanostructure	Capacitance performance	Description of the mothod
Adv. Funt. Mater., 2012. 20. 1680-1686	Co_3O_4 hollow spheres	700 mAh g^{-1} at 30th cycle	Hydrothermal treatment followed by calcination process.
Mate. Lett., 91 (2013) 291-293	Co_3O_4 nanoparticles	652 mAh g^{-1} at 50th cycle	Cobalt nitrate hexahydrate and PVP were mixed and then heated to high temperature for 24h.
Solid State Sciences 14 (2012) 451-455	chrysanthemum-like Co_3O_4 architectures	380 mAh g^{-1} at 20th cycle	Hydrothermal route and a subsequent calcination process.
Journal of Solid State Chemistry 183 (2010) 600-605	flower-like Co_3O_4	150 mAh g^{-1} at 20th cycle	Cobalt nitrate hexahydrate, sodium hydroxide and succinic acid mixed and then heated to high temperature.
Chem. Commun., 2011.47.3469-3471	foam-like freestanding Co_3O_4 nanosheets	750 mAh g^{-1} at 20th cycle	Co to grow a $Co(OH)_2$, followed by thermal treatment to form mesoporous Co_3O_4.
Chem. Commun., 2011.47.12280-12282	Co_3O_4 self-stacked nanosheets	920mAh g^{-1} at 40th cycle	Self-stacked Co_3O_4nanosheets were obtained by a solvothermal method in the presence of (PVP) and water followed by a calcination treatment.
J. Mater. Chem., 2011.21.17998-18002	Co_3O_4-C core-shell sphere	720 mAh g^{-1} at 40th cycle	Cobalt(II) acetate tetrahydrate and sodium citrate were added to ethylene glycol (EG) followed by hydrothermal treatment, Finally, calcination treatment.

Table S1 shows a complete table of comparison about the capacitance performance in the literatures. As shown in Table S1, the reported capacitance performance is varied from 150 to 920 mAh g^{-1}, with a common value of ~700 mAh g^{-1}, which is a little lower than

our capacitance performance of 720 mAh g^{-1}. However, Costly equipment and multisteps increase the cost and are time consuming, which significantly hinders the process scale-up. Therefore, more efforts should still be focused on controlling synthesis of Co_3O_4 nanostructures on the substrate in a convenient way. And it should be pointed out that in this manuscript, besides the capacitance performance of Co_3O_4, we more focused on developing a universal strategy for controlled synthesis of porous metal oxide and carbon hybrid nanosheet arrays directly on various substrates, especially on the conductive flexible subtracts, which is rarely reported and shows the originality of our work. And our results demonstrated that the proposed method is very convenient for direct growth porous metal oxides and carbon hybrid nanosheet arrays on conductive flexible subtract such as carbon cloth, which is promising for the flexible electronics technology of energy storage devices. Other metal oxides which can achieve much higher lithium battery performance or good for other applications will be the further studied with this method in the future.